Effect of adaptive cruise control systems on traffic flow

L. C. Davis*
Physics Department, University of Michigan, Ann Arbor, Michigan 48109, USA
(Received 27 October 2003; revised manuscript received 22 January 2004; published 4 June 2004)

The flow of traffic composed of vehicles that are equipped with adaptive cruise control (ACC) is studied using simulations. The ACC vehicles are modeled by a linear dynamical equation that has string stability. In platoons of all ACC vehicles, perturbations due to changes in the lead vehicle's velocity do not cause jams. Simulations of merging flows near an onramp show that if the total incoming rate does not exceed the capacity of the single outgoing lane, free flow is maintained. With larger incoming flows, a state closely related to the synchronized flow phase found in manually driven vehicular traffic has been observed. This state, however, should not be considered congested because the flow is maximal for the density. Traffic composed of random sequences of ACC vehicles and manual vehicles has also been studied. At high speeds ($\sim$30 m/s) jamming occurs for concentrations of ACC vehicles of 10% or less. At 20% no jams are formed. The formation of jams is sensitive to the sequence of vehicles (ACC or manual). At lower speeds ($\sim$15 m/s), no critical concentration for complete jam suppression is found. Rather, the average velocity in the pseudojam region increases with increasing ACC concentration. Mixing 50% ACC vehicles randomly with manually driven vehicles on the primary lane in onramp simulations shows only modestly reduced travel times and larger flow rates.

DOI: 10.1103/PhysRevE.69.066110 PACS number(s): 89.40.−a, 45.05.+x

I. INTRODUCTION

Most of the literature on traffic theory, even the modern literature, has focused on describing manually driven vehicles [1–18]. However, reports on vehicles with adaptive cruise control (ACC) are now appearing in anticipation of the widespread use of such driver assistance systems [19–25]. In an ACC vehicle the delay due to driver reaction time is eliminated and a control system attempts to keep the vehicle at the desired headway to the preceding vehicle. Through the use of radar (or other signaling means) and sensors, the range and rate of change of range can be measured accurately and essentially instantaneously. The principal element of the control algorithm is the headway policy. In the present work, the "constant-headway time" policy is chosen because of its known stability [23]. The scientific questions posed by the introduction of ACC systems are: (1) What traffic phases can one expect in an all-ACC scenario? (2) In mixed traffic consisting of both ACC and manual vehicles, to what extent (if at all) can congestion be reduced by increasing the fraction of ACC vehicles? Of course traffic engineers are interested in the benefits, such as possible reduced travel times, and the impact on safety of extensive use of driver-assistance systems.

There are now several papers making use of simulations to study the effects of ACC vehicles. So far the results appear to be mixed—some benefits and some disadvantages. In small-scale simulations, Kikuchi, Uno, and Tanaka [24] found that ACC vehicles "can shorten the process of achieving stability." Likewise, Kerner [22] found that ACC vehicles suppress wide moving jams and thus promote stability. On the downside, however, he also found that in some cases ACC vehicles could induce congestion at bottlenecks. In detailed simulations of a section of the German autobahn A8-East, Treiber and Helbing [21] reported that if 20% of vehicles were equipped with ACC, nearly all of the congestion was eliminated. Even for only 10%, they found that the additional travel time due to traffic jams was reduced by more than 80%. Bose and Ioannou [25] showed that for mixed traffic, where semiautomated vehicles have a higher flow rate at a given density than manually driven vehicles, the flow-density curve should fall between the curves for all semiautomated and all manual. In their calculations, for equal mixtures of semiautomatic and manual vehicles, only marginal travel time reductions (at best) were noted. Although in stop-and-go traffic the delay at standstill was found to be lower than for all manually driven vehicles.

From the scientific perspective, the dynamics of ACC vehicles differ from those of manual vehicles, which are for the present purposes described by the three-phase model of traffic due to Kerner and collaborators [3,4,8]. This theory postulates that equilibrium states occupy a region of the two-dimensional flow-density space. Many other traffic models have assumed that in equilibrium there is a unique relationship on average between vehicle velocity ν and headway h,

$$\nu = f(h). \tag{1}$$

In flow-density space these solutions lie on the curve (the fundamental diagram) given by

$$q(\rho) = \rho f(h), \tag{2a}$$

$$\rho = 1/h. \tag{2b}$$

It is expected that ACC systems will have these characteristics. On the other hand, in the three-phase model of manually driven vehicles there are equilibrium solutions of the form

$$\nu_n(t) = f(h),$$

*Email: ldavis7@peoplepc.com

$$\Delta x_n(t) \geqslant h \tag{3}$$

for the nth vehicle. Even though every vehicle may travel at the same velocity, the headway to the preceding vehicle $\Delta x_n(t)$ can be any value greater than h within limits. The flow is

$$q = \overline{\rho} f(h), \tag{4}$$

where the average density is

$$\overline{\rho} = \frac{1}{\langle \Delta x_n \rangle} \leqslant \frac{1}{h}. \tag{5}$$

The symbol $\langle \Delta x_n \rangle$ stands for the average headway. These solutions lie on or below the $q(\rho)$ curve.

The purpose of the present work is to study how the introduction of ACC vehicles, with different dynamics, influence traffic flow, especially in relation to congestion. It is organized as follows. Section II describes the dynamics of ACC vehicles in more detail and shows that spontaneous jam formation does not occur. Section III is devoted to simulations in an all-ACC scenario with an onramp and possible transitions to the synchronized flow (SF) phase. Sections IV and V consider mixed traffic. Section IV pertains to single-lane simulations and jam formation, while Sec. V treats multilane simulations. Section VI summarizes the conclusions of this study.

II. DESCRIPTION OF ACC DYNAMICS

In this section, I describe the dynamics of ACC vehicles. Let the vehicles be numbered $n=1-N$ from front to rear of the platoon. The lead vehicle corresponds to $n=0$ and its velocity $v_0(t)$ is arbitrary. The dynamics of the ideal adaptive cruise control system can be modeled by the following equation [19–25]:

$$\tau \frac{dv_n(t)}{dt} + v_n(t) = V(\Delta x_n(t), \Delta v_n(t)), \tag{6}$$

where the distance between the nth vehicle and the preceding one is

$$\Delta x_n(t) = x_{n-1}(t) - x_n(t). \tag{7}$$

This quantity is the range (including vehicle length) and its rate of change is

$$\Delta v_n(t) = v_{n-1}(t) - v_n(t). \tag{8}$$

Vehicle response is modeled by first-order dynamics with a time constant τ, which is typically 0.5–1.0 s. The function V is specified below.

The desired headway according to the constant-time headway policy is given by

$$\Delta x_n^{desired}(t) = h_d v_n(t) + D, \tag{9}$$

where h_d is the headway time, generally about 1.0 s, and D is a constant length, slightly longer than the length of a vehicle. Throughout this paper, D is taken to be 7 m. Thus I take V (which should be linear) as

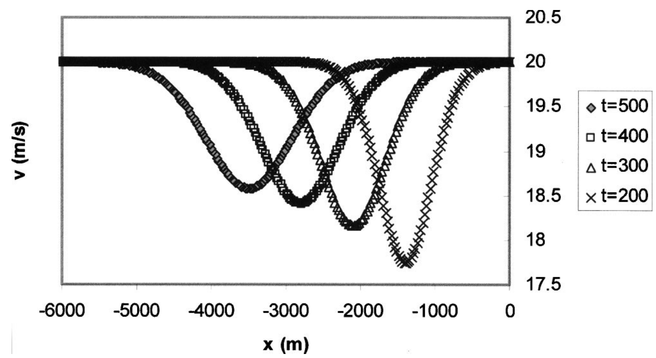

FIG. 1. Velocity of ACC vehicles vs position at various times (200, 300, 400, 500 s) responding to a perturbation due to the lead vehicle that was stopped for 2 s before accelerating to 20 m/s.

$$V = \frac{1}{h_d}[\Delta x_n(t) - D] + \beta \Delta v_v(t). \tag{10}$$

The coefficient of the rate of change of the range is β and remains to be specified. The maximum velocity constraint requires $V < V_{max} = 35$ m/s, which is imposed by constraining velocities numerically to remain at or below 35 m/s in the simulations. Backing up is forbidden as well. One way to determine β is to choose it to minimize the velocity error, which is defined as the difference between the actual velocity and the desired velocity.

$$\varepsilon_n(t) = v_n(t) - V_d(\Delta x_n(t)), \tag{11}$$

where the desired velocity is

$$V_d(\Delta x) = \frac{1}{h_d}(\Delta x - D). \tag{12}$$

If I take $\beta = \tau / h_d$, it is straightforward to show that (assuming the constraints are not violated)

$$\tau \dot{\varepsilon}_n(t) + \varepsilon_n(t) = 0. \tag{13}$$

Hence,

$$\varepsilon_n(t) = \varepsilon_n(0) e^{-t/\tau}, \tag{14}$$

which implies the velocity error vanishes for $t \gg \tau$ and

$$v_n(t) = V_d(\Delta x_n(t)) \tag{15}$$

or that the headway error

$$\Delta x_n(t) - h_d v_n(t) - D \to 0. \tag{16}$$

Note this choice for β gives $V(\Delta x(t), \Delta v(t)) = V_d(\Delta x(t) + \tau \Delta v(t))$. The effective headway includes anticipation of the change during the time interval t to $t+\tau$.

In simulations to demonstrate these dynamics, which are presented in Fig. 1, 600 cars were started at $t=0$ with velocity 20 m/s and headway 27 m corresponding to $h_d=1$ s. The lead vehicle was at zero velocity for 2 s and then accelerated to 20 m/s in 4 s, remaining at a constant velocity thereafter. [Throughout the paper $\tau=0.5$ s.] To demonstrate that a perturbation does not grow with increasing n, I show in Fig. 1 a

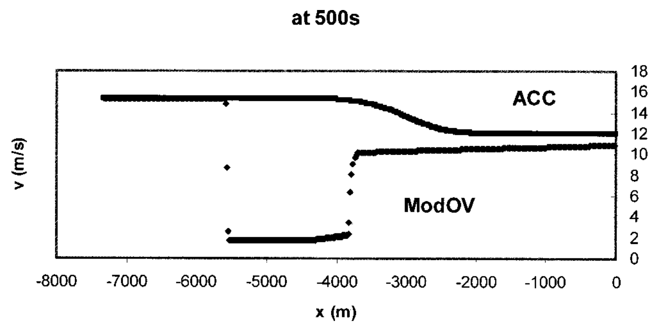

FIG. 2. A comparison of the velocity of ACC vehicles (upper trace) and manually driven vehicles (lower trace) at 500 s as a function of position. In response to the lower velocity (12 m/s) of the lead vehicle, manual vehicles initially at the critical density (0.04 vehicles/m for velocity 15.34 m/s) form a jam of nearly 2 km length, whereas the ACC vehicles make a smooth transition. The manual vehicles are described by the modified optimal velocity model (ModOV).

snapshot of all vehicles at various times. The dip in velocity (a response to the lead vehicle's velocity profile) becomes smaller with increasing car number. *A perturbation does not grow with successive vehicles (larger n).*

Liang and Peng [19,20] proved a relevant conclusion about stability of a platoon of vehicles (called string stability). They showed that the magnitude of the transfer function relating Δx_n to Δx_{n-1} does not exceed unity if the following holds:

$$K_2 > \frac{2 - K_1 h_d^2}{2h_d}, \tag{17}$$

where

$$K_1 = \frac{1}{\tau h_d} \tag{18}$$

and

$$K_2 = \frac{\beta}{\tau}. \tag{19}$$

If I take $\beta = \tau/h_d$, the inequality is satisfied for any positive τ and h_d. If $\beta=0$, then $2\tau < h_d$ is required for stability.

A simulation demonstrates the stability against the formation of a traffic jam. The initial conditions are given by $\Delta x_n(0) = 25$ m and $v_n(0) = 15.34$ m/s. The time headway $h_d = 1.1734$ s and $\beta = \tau/h_d$. These parameters are convenient for comparison to a simulation using the modified optimal velocity (ModOV) model [27,28], which satisfies the postulate of the three-phase theory [4,8], to describe vehicles without adaptive cruise control. (See the Appendix for a description of the ModOV model.) The lead vehicle velocity $v_0(t) = 12$ m/s. The comparison is shown in Fig. 2. Clearly the jam found for manually driven vehicles does not form in the simulations for ACC vehicles. Throughout this paper, the delay time for manual vehicles is $t_d = 0.75$ s.

Liang and Peng [19,20] defined a performance index that takes into account not only the magnitudes of the headway error and velocity differences $\Delta v_n(t)$, but also the accelerations. Depending on how they weighted each contribution, they obtained different numerical values for K_1 and K_2 from simulations. However, generally they found that $\beta > \tau/h_d$ provides a more favorable index.

Similarly, for a circular road [periodic boundary conditions for which $v_0(t)$ is replaced by $v_N(t)$], Li and Shrivastava [23] proved asymptotic stability with an exponential convergence rate. That is, if there are N vehicles on a length L of highway (i.e., the circumference of the circle), $\Delta x_n(t) \to L/N$ quickly for all n and arbitrary initial conditions.

Finally, Konishi, Kokame, and Hirata [26] have proposed a delayed-feedback control that has been shown to be successful in controlling chaotic systems. Applied to a linear traffic model with a constant time headway policy [but without the $\beta \Delta v_n(t)$ term], the control scheme was shown to suppress traffic jams. The continuous form of the control law is given by adding a term $u_n(t)$ so that the dynamics is described by

$$\tau \frac{dv_n(t)}{dt} + v_n(t) = V_d(\Delta x_n(t)) + u_n(t), \tag{21}$$

where

$$u_n(t) = k[\Delta x_n(t) - \Delta x_n(t - \tau_d)] \tag{22}$$

and τ_d is a delay time, chosen to optimize the response. To first order, one can write

$$u_n(t) = k[\Delta \dot{x}_n(t)\tau_d + \cdots], \tag{23}$$

which gives the same form for Eq. (21) as Eq. (6) with Eq. (10) substituted.

III. ONRAMP SIMULATIONS

Jams are only one phase of traffic congestion. The linear ACC model has been shown to be stable against formation of jams, but it has not been established if it is resistant to other forms of congestion, such as the synchronized flow (SF) phase. Let us consider an onramp where transitions to SF are often observed. (Only multilane simulations in scenarios with all ACC vehicles are considered in this section.)

Two lanes come together in a merge region $-d_{merge} < x < 0$ where vehicles in lane 2 can merge into lane 1, which continues on beyond $x > 0$. The rules for merging are the same as given by Davis [28] with safe headways for ACC vehicles determined from Eq. (12) (without any time delays). Random choosing of vehicles to attempt merging is used in the simulations. For simplicity no limits on acceleration or deceleration are imposed because unrealistic values generally occur only during merging. Since oncoming vehicles in lane 1 do not attempt to accommodate vehicles changing lanes to make merging smoother, these are compensating effects.

The initial conditions are as follows: vehicles in lane 1 occupy sites spaced at equal intervals of $h = 42$ m$(x = -jh, j = 1, 2, \ldots)$ with probability $p_1 = 0.8$; those in lane 2 occupy

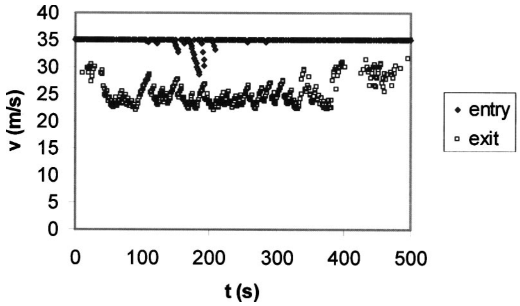

FIG. 3. Velocities of ACC vehicles as a function of time at the beginning of the merge region ("entry") in both lanes and just beyond the downstream end of the merge region ("exit"). The length of the merge region is 500 m. The total incoming flow is at capacity for the initial headway and velocity (42 m and 35 m/s, the maximum allowed velocity) with 80% in lane 1 and the remaining 20% in lane 2, the onramp. Parameter values: $\tau=\tau_1=0.5$ s and $h_d=1.0$ s.

similar sites with probability $p_2=0.2$. The headway time constant is taken to be $h_d=1$ s, so the initial velocity of all vehicles is 35 m/s. The length of the merge region is $d_{merge}=500$ m. Vehicle velocities at the entry to the merge region ($x=-500$ m) are plotted as they pass. Likewise, vehicle velocities just beyond the exit from the merge region ($x=25$ m) are plotted. Whereas the entering vehicles mostly travel with the initial velocity of 35 m/s, the exiting vehicles leave at a range of velocities around 25 m/s. This is due to merging at small velocities near the end of the merge region. See Fig. 3. Downstream the vehicles accelerate to the lead vehicle velocity of 35 m/s.

The rates of vehicles passing "entry" and "exit" are plotted as a function of time in Fig. 4. Twenty-car averages are shown. The rate in lane 1 fluctuates around the initial rate of 2/3 vehicles/s and in lane 2 around 1/6 vehicles/s. The exit rate is near or above the full capacity of a single lane, 5/6 vehicles/s. Since the exit rate is approximately the sum of the entry rates, no significant accumulation of vehicles occurs in the merge region. No evidence of synchronized flow was found in this simulation. Only a small region of reduced velocity occurred at the downstream end of the merge region. It did not appear to grow in size. A calculation for manually driven cars under similar conditions produces the SF phase.

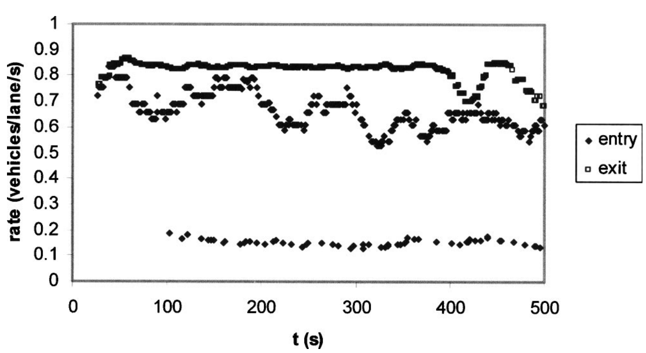

FIG. 4. Flow rate at the entry and exit of the merge region. The lowest trace is the flow on the onramp. Parameters and initial conditions are the same as in Fig. 3.

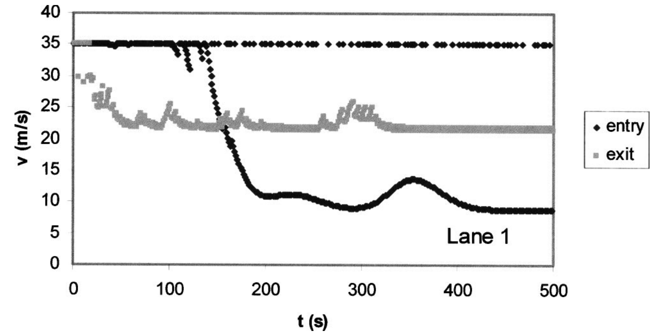

FIG. 5. Velocities of ACC vehicles as a function of time for larger incoming flow (30% of capacity) on the onramp with lane 1 flow at 80% capacity.

Increasing the incoming rate in lane 2 by making $p_2=0.3$ produces a dramatic change in the velocity of vehicles in lane 2. Between 100 and 200 s the velocity at the entry drops from 35 m/s to 10–15 m/s. The flow in lane 1 drops, but the exit flow remains at capacity. Flow in either lane 1 or lane 2 (or both) at entry must drop because the total incoming flow exceeds the maximum for the single-lane exit. The alternative would be for a jam (where the velocity drops to near zero) to form in either or both incoming lanes. See Figs. 5 and 6.

If the rate of incoming vehicles is increased substantially beyond the capacity of a single lane, a transition to the SF phase is observed in both lanes, as shown in the following simulation (Fig. 7). The initial conditions (which mimic those of Davis [28] for manually driven vehicles) are $p_1=1$ with $v=29.77$ m/s and $h=48.8$ m (22% larger than the constant headway time value of 40 m) and $p_2=0.9$ with $v=29.77$ m/s and $h=44$ m (10% larger than the constant headway time value). For comparison purposes, a speed limit of $v_{max}=29.77$ m/s was imposed and $h_d=1.1085$ s in this simulation. The length of the merge region is 500 m. The observation point for "entry" is at $x=-500$ m. A clear transition to a SF phase can be seen between 100 and 200 s. The transition in lane 2 reaches a lower velocity, 2.4 m/s compared to 7.7 m/s in lane 1.

To establish that the flow transformed into the SF phase, consider the flow rate versus density plot (q versus ρ) shown in Fig. 8. The rate for lane 1 begins on the free flow line

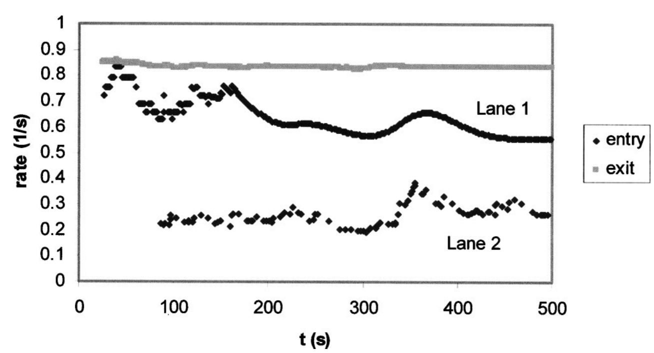

FIG. 6. Flow rates for individual lanes as a function of time for incoming flow that is 30% of capacity on the onramp and at 80% capacity in lane 1. Parameters are the same as in Fig. 5.

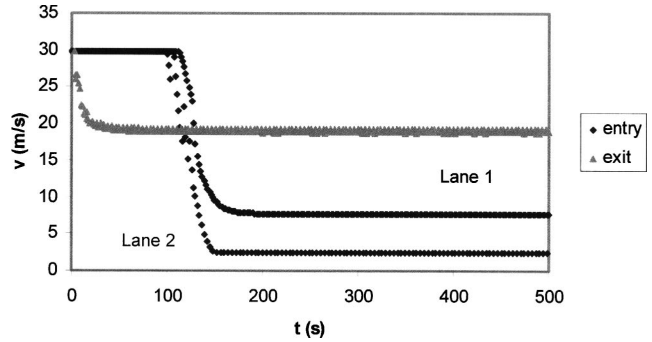

FIG. 7. Velocities of ACC vehicles as a function of time for large incoming flow rates, approximately 80% of capacity in each lane at the initial velocity of 29.77 m/s. Here h_d=1.1085 s and a speed limit of 29.77 m/s was imposed.

($q=\rho\nu_{max}$) and transforms to the downward sloping portion of the ideal rate line: $q=(1-\rho D)/h_d$. The exit rate is above the ideal rate line indicating a metastable condition. Further downstream, equilibrium was approached.

It should be noted that the rate in the SF phase in each lane goes to the maximum rate for the given final densities (points on the downward sloping line). Thus flow should not be regarded as congested. This is in contrast to flow in the corresponding manual-driver simulations, where the rate falls significantly below the line.

Other simulations (not displayed) showed that if the combined incoming flux of vehicles did not exceed the capacity of the single outgoing lane, then no significant congestion occurred. Free flow was found for any combination of incoming rates (q_1 in lane 1 and q_2 in lane 2) tried so long as the following condition held:

$$q_1 + q_2 < q_{max}, \tag{24}$$

where the maximum single-lane flow rate is

$$q_{max} = \frac{\nu_{max}}{\nu_{max} h_d + D}. \tag{25}$$

For an all ACC system, when limits on acceleration or deceleration are imposed an effective scheme to merge vehicles smoothly is required for Eqs. (24) and (25) to hold.

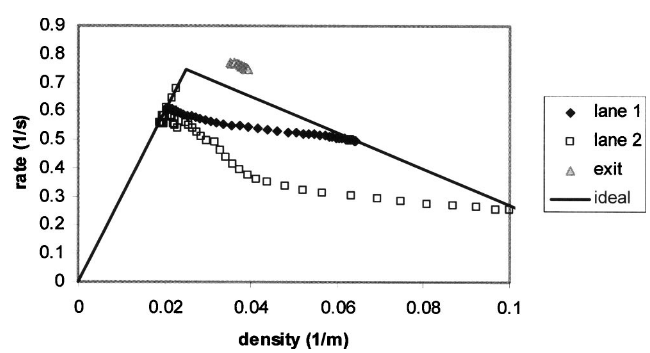

FIG. 8. Flow rate q in each lane vs density ρ and ideal rate for ν_{max}=29.77 m/s and h_d=1.1085 s. The incoming flow rates in each lane are approximately 80% of the capacity of a single lane.

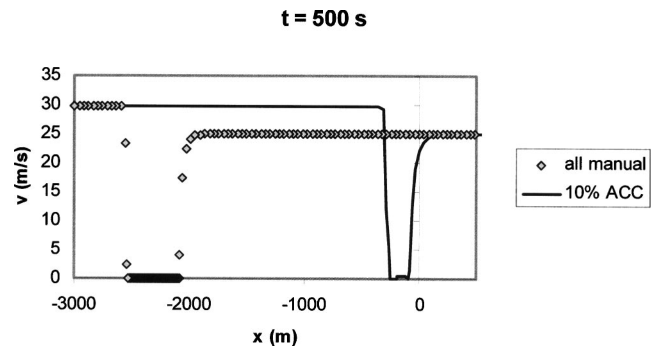

FIG. 9. Velocity vs position of vehicles at t=500 s. With no ACC vehicles and with 10% ACC randomly mixed in with manual vehicles, a jam is formed due to encountering a slower moving lead vehicle (traveling at 25 m/s). In this example, if 20% of the vehicles were ACC, no jam was formed. Initially all vehicles in the platoon were traveling at 29.77 m/s with a headway of 40 m. The parameters were $\tau=\tau_1$=0.5 s, h_d=1.1085 s, and t_d=0.75 s (manual-driven vehicles only).

IV. SINGLE-LANE SIMULATIONS OF MIXED FLOW

The effect of mixing ACC vehicles with manually driven vehicles is explored in this section. Only the results from single-lane simulations are discussed here; multilane simulation is the subject of Sec. V. Mixed flow is of interest because the introduction of driver-assistance systems into the fleet of vehicles on highways will be gradual over time (on the scale of years or perhaps decades).

Treiber and Helbing [21] have reported that fitting 20% of vehicles with driver-assistance systems makes congestion vanish in simulations of a section of the autobahn A8-East. In Fig. 9, results for mixing ACC vehicles randomly with manually driven vehicles are presented. The initial conditions were h=40 m with ν=29.77 m/s on a single-lane highway. The lead vehicle traveled at a constant speed of 25 m/s. The headway time was h_d=1.1085 s, which gives the same initial headways for ACC and manual vehicles. For no ACC vehicles, a jam is formed that extends for approximately ½ km with the upstream edge at $x=-2.5$ km at t=500 s. Calculations were done with the ModOV [27,28] model for the manual vehicles. With 10% ACC vehicles, the jam was half as long and moved upstream more slowly. In this instance, equipping vehicles with ACC appears to have no significant benefit on suppressing jams until the percentage is larger than 10%. No jam was formed at 20% ACC, however, in agreement with the findings of Treiber and Helbing.

To explore the region between 10% ACC, where a jam was formed, and 20% where the jam was suppressed, the following simulations were performed. The parameters were the same as for Fig. 9. In Fig. 10, the results for two sequences with ~13% ACC are shown. This is a striking case of how the details of the random sequence influence whether or not a jam is formed. *Merely changing one manual vehicle to an ACC vehicle (the 188th vehicle) prevents the formation of a jam*.

The sensitivity of the results to the sequence of ACC and manual vehicles is further illustrated by considering periodic arrays of k manual vehicles followed by one ACC vehicle.

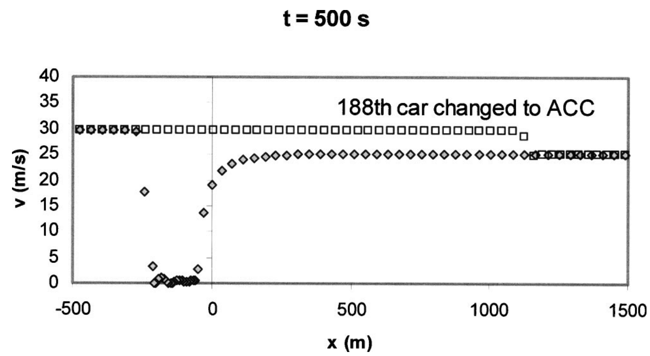

FIG. 10. Velocity vs position at $t=500$ s for two sequences of manual and ACC vehicles (approximately 13% concentration) for the initial conditions and parameters of Fig. 9. The change of a single manual vehicle (the 188th) to ACC suppressed the formation of a jam (square symbols).

For the parameters and initial conditions of Figs. 9 and 10, simulations demonstrated that k can be as large as 15 without a jam forming. These results differ from those of Kurata and Nagatani [29] who analyzed binary mixtures of manual and automated vehicles in periodic and random sequences. They found that moving in groups of one manual and n automated vehicles ($n=1-4$) stabilized and enhanced flow. For random sequences of manual and automated vehicles, they found that jamming transitions depended weakly on the random configuration in contrast to the present results. Their vehicular models were substantially different from those used here and the simulations were performed on a circular track rather than an endless road.

The critical region of the ModOV model, like that of the original OV model [1], is near the headway Δx^0 (the inflection point in the OV function), which is 25 m for the parametrization used in this paper. Jam formation is the most likely near this headway for manual vehicles. In Fig. 11, results are presented for initial conditions $h=25$ m with $\nu=15.34$ m/s and 0, 10, and 50% ACC vehicles encountering a lead vehicle traveling at 13 m/s. The headway time for the ACC vehicles was $h_d=1.1735$ s. The plot of velocity versus position at $t=500$ s reveals that jam formation is suppressed by ACC vehicles at high enough concentration.

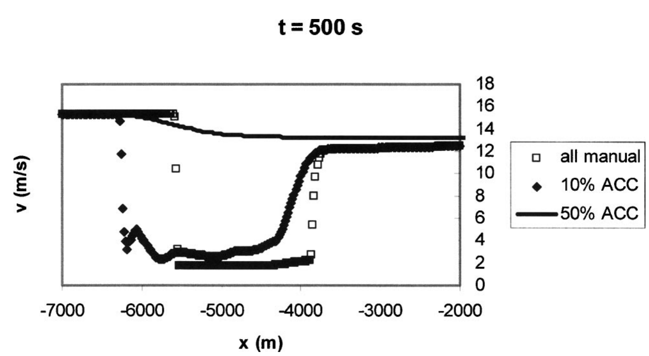

FIG. 11. Velocity vs position at $t=500$ s for initial conditions $h=25$ m with $\nu=15.34$ m/s and 0, 10, and 50% ACC vehicles encountering a lead vehicle traveling at 13 m/s. The headway time for the ACC vehicles was $h_d=1.1735$ s.

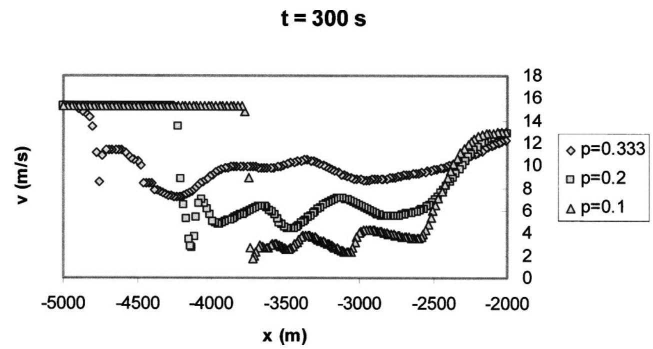

FIG. 12. Velocity vs position at $t=300$ s for ACC vehicle concentration in lane 1 of $p=0.1$, 0.2, and 1/3. Parameters were the same as in Fig. 11.

Simulations displayed in Fig. 12 show that as the ACC concentration is increased from $p=0.1$ to 1/3, the velocity in the pseudojam region increased gradually (from 4 m/s at 10% to 9 m/s at $p=1/3$), rather than abruptly going from the formation of a jam to the absence of a jam as in Figs. 9 and 10. That is, it does not appear that a critical concentration exists. The pseudojam region also widened with increasing ACC concentration. For $p=1/3$ the average density (~ 0.05 m^{-1}) and average velocity (~ 9 m/s) or flow rate (0.45 s^{-1}) are more like the values for the single-lane version of synchronized flow than for a jam [28].

V. MULTILANE SIMULATIONS OF MIXED TRAFFIC

In this section, the effect of randomly mixing ACC with manually driven vehicles on lane 1 in onramp simulations is examined. The vehicles on lane 2 were all manually driven and obeyed the merging rules of Ref. [28]. Two cases are considered: (a) all manual and (b) 50% ACC. In the simulations, flow in lane 1 was initially 80% of capacity and flow in lane 2 was 20%. Vehicles in lane 2 were offset initially to more negative x by 500 m. The headway time was 1.1085 s,

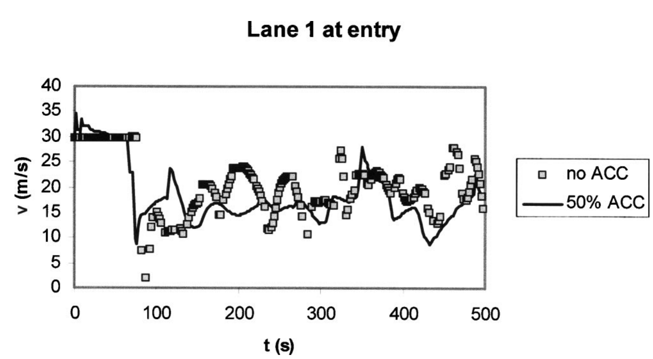

FIG. 13. Velocity vs time for vehicles in lane 1 passing the upstream end of the merge region. The squares correspond to all manual vehicles and the solid line is for 50% of the vehicles in lane 1 randomly taken to be ACC. Vehicles in lane 2 (the onramp) were all manual. The headway time was $h_d=1.1085$ s. The delay for manually driven vehicles was $t_d=0.75$ s. The initial conditions were $h=40$ m with $\nu=29.77$ m/s, $p_1=0.8$ and $p_2=0.2$.

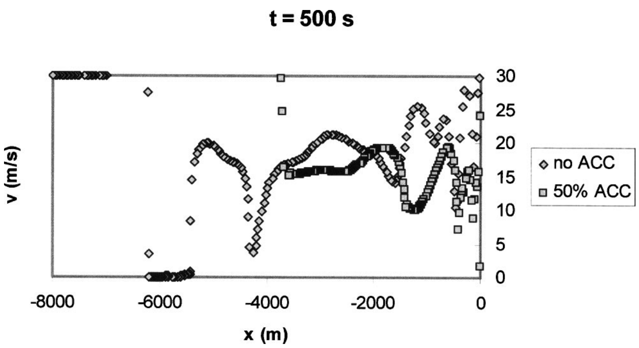

FIG. 14. Velocity vs position at $t=500$ s for the initial conditions and parameters of Fig. 13.

which made the initial headways identical for ACC and manual vehicles. The lead vehicle traveled at 33 m/s. Figure 13 shows the velocity of vehicles in lane 1 passing the upstream end of the merge region at $x=-500$ m. The average velocity for $100 < t < 500$ s was determined to be: (a) 19.1 m/s for all manual and (b) 16.5 m/s for the 50% ACC case. However, the average distance traveled by the first 400 vehicles in the first 400 s was larger for (b) by approximately 1 km.

As shown in Fig. 14, the introduction of 50% ACC vehicles in lane 1 suppressed the formation of a jam upstream of the merge region. For all manually driven vehicles the jam extended for more than 0.5 km at 500 s. So, in case (b) the average velocity of vehicles in lane 1 at entry was less than in (a), but no jam was formed. The average rate of flow in lane 1 was somewhat higher in case (b) (approximately 0.55 compared to 0.45 vehicles/s). At $x=25$ m, the outgoing rate was (a) 0.604 and (b) 0.666/s.

If $h_d=0.8$ s and the initial headway to the preceding vehicle adjusted accordingly for ACC vehicles (they follow more closely), the average velocity increased slightly from 16.5 to 17.1 m/s. Flow at the exit improved to 0.712 vehicles/s, mostly because the initial density in lane 1 was larger.

VI. CONCLUSIONS

Two questions were addressed in this paper. The first concerned traffic phases that exist in a scenario with all ACC vehicles. Simulations done with a dynamical model where the desired velocity is proportional to the effective headway $\Delta x+\tau\Delta v$ showed that jams do not form. Multilane simulations where one lane is an onramp showed that free flow is maintained in both lanes if the total incoming flow does not exceed the capacity of the single outgoing lane. When incoming flow is larger, a phase similar to the synchronized flow phase of the three-phase model is observed. However, it should not be considered congested because the flow is on the fundamental diagram of rate versus density. That is, the flow is the maximum value (at equilibrium) for the observed density.

The second question dealt with traffic in which ACC vehicles are randomly mixed in with manually driven vehicles. Single-lane simulations showed that a concentration of 10% ACC vehicles is insufficient to prevent jams at high velocities (~30 m/s). However, jams are suppressed by 20% ACC. The formation of jams was found to be sensitive to the sequence of vehicle types (ACC or manual) in random and periodic sequences. At moderate velocities (~15 m/s), the effect of increasing ACC concentration is different. In this case increased concentration does not prevent jamming, but instead increases the average velocity in the pseudojam region. Multilane simulations with a random 50% concentration of ACC vehicles in lane 1 and all manual vehicles on the onramp demonstrated only modest improvement over having all manually driven vehicles. The average velocity in lane 1 at entry to the merge region was slightly less for the 50% case, although the average distance traveled for a given time was bigger. The throughput was somewhat larger for the mixed flow, especially for short ACC headway times.

No unusual nonequilibrium or chaotic flows were found (although the simulations presented here were not exhaustive of all possible situations). One potential problem with merging was identified, however. Since ACC vehicles closely maintain the equilibrium or desired headways for the vehicles' velocities, the ability of manually driven vehicles to merge might be hindered by the lack of suitable safe gaps. Also, vehicles operating in an ACC mode do not "give way" like some human drivers do when a vehicle enters from an onramp.

ACKNOWLEDGMENTS

I thank Professor Huei Peng for a useful discussion.

APPENDIX

The dynamical equations for the nth vehicle in the ModOV model are

$$\tau\frac{dv_n(t)}{dt} + v_n(t) = V_{desired}, \tag{A1}$$

where

$$V_{desired} = V_{OV}, \quad V_{OV} < v_n(t), \tag{A2a}$$

$$= \min\{V_{OV}, v_{n-1}(t-t_d)\}, \quad V_{OV} > v_n(t), \tag{A2b}$$

and

$$V_{OV} = V(\Delta x_n(t-t_d) + t_d\Delta v_n(t-t_d)), \tag{A3}$$

where

$$V(\Delta x_n) = V_0\{\tanh[C_1(\Delta x_n - \Delta x^0)] + C_2\}, \quad \Delta x_n = x_{n-1} - x_n. \tag{A4}$$

At large headway,

$$V_{desired} = \alpha\ \nu_{n-1}(t - t_d) + (1 - \alpha)V_{OV}, \quad \text{(A5)}$$

where

$$\alpha = \exp(1 - \Delta/L), \quad \Delta > L \quad \text{(A6)}$$

and

$$\Delta = \Delta x_n(t - t_d) + t_d \Delta \nu_n(t - t_d), \quad \text{(A7)}$$

provided $V_{OV} > \nu_n(t)$. I take $L = 100$ m. Other parameters are $C_1 = 0.86/\mathrm{m}$, $C_2 = 0.913$, $\Delta x^0 = 25$ m, and $V_0 = 16.8$ m/s. See Ref. [2].

[1] M. Bando, K. Hasebe, A. Nakayama, A. Shibata, and Y. Sugiyama, Phys. Rev. E **51**, 1035 (1995).
[2] Y. Sugiyama, in *Workshop on Traffic and Granular Flow*, edited by D. E. Wolf, M. Schreckenber, and A. Bachem (World Scientific, Singapore, 1996), p. 137.
[3] B. S. Kerner and H. Rehborn, Phys. Rev. Lett. **79**, 4030 (1997).
[4] B. S. Kerner, Phys. Rev. Lett. **81**, 3797 (1998).
[5] D. Helbing and M. Treiber, Phys. Rev. Lett. **81**, 3042 (1998).
[6] D. Helbing, A. Hennecke, and M. Treiber, Phys. Rev. Lett. **82**, 4360 (1999).
[7] M. Treiber and D. Helbing, e-print cond-mat/9901239.
[8] B. S. Kerner, Transp. Res. Rec. **1678**, 160 (1999).
[9] T. Nagatani, Phys. Rev. E **61**, 3534 (2000).
[10] M. Treiber, A. Hennecke, and D. Helbing, Phys. Rev. E **62**, 1805 (2000).
[11] D. Helbing, Rev. Mod. Phys. **73**, 1067 (2001).
[12] B. S. Kerner, Phys. Rev. E **65**, 046138 (2002).
[13] B. S. Kerner and S. L. Klenov, J. Phys. A **35**, L31 (2002).
[14] B. S. Kerner, S. L. Klenov, and D. E. Wolf, J. Phys. A **35**, 9971 (2002).
[15] Boris S. Kerner, Transp. Res. Rec. **1802**, 02-2918 (2002).
[16] Boris S. Kerner, e-print cond-mat/0211684.
[17] Boris S. Kerner and Sergey L. Klenov, Phys. Rev. E **68**, 036130 (2003).
[18] *Transportation and Traffic Theory in the 21st Century*, edited by Michael A. P. Taylor (Pergamon, Amsterdam, 2002).
[19] ChiYing Liang and Huei Peng, Veh. Syst. Dyn. **31**, 313 (1999).
[20] ChiYing Liang and Huei Peng, JSME Int. J., Ser. C **43**, 671 (2000).
[21] Martin Treiber and Dirk Helbing, e-print cond-mat/0210096.
[22] Boris S. Kerner, e-print cond-mat/0309017.
[23] Perry Y. Li and Ankur Shrivastava, Transp. Res., Part C: Emerg. Technol. **10**, 275 (2002).
[24] Shinya Kukuchi, Nobuhiro Uno, and Mitsura Tanaka, J. Transp. Eng. **129**, 146 (2003).
[25] Arnab Bose and Petros Ioannou, Transp. Res., Part C: Emerg. Technol. **11**, 439 (2003).
[26] Keiji Konishi, Hideki Kokame, and Kentaro Hirata, Phys. Rev. E **60**, 4000 (1999); K. Konishi, H. Kokame, and K. Hirata, Eur. Phys. J. B **15**, 715 (2000).
[27] L. C. Davis, Physica A **319**, 557 (2003).
[28] L. C. Davis, Phys. Rev. E **69**, 016108 (2004).
[29] Shingo Kurata and Takashi Nagatani, Phys. Rev. E **64**, 016106 (2001).